

# Spontaneous Graphitization of Ultrathin Cubic Structures: A Computational Study

Pavel B. Sorokin,<sup>†,‡,§</sup> Alexander G. Kvashnin,<sup>‡,§</sup> Zhen Zhu,<sup>†</sup> and David Tománek<sup>\*,†</sup>

<sup>†</sup>Physics and Astronomy Department, Michigan State University, East Lansing, Michigan 48824, United States

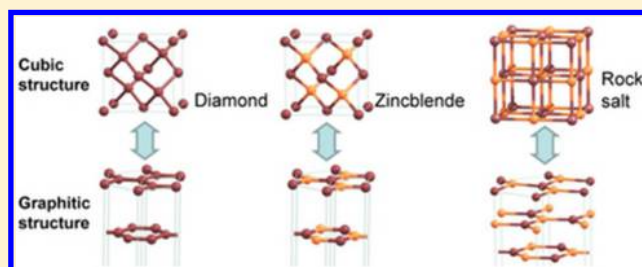
<sup>‡</sup>FSBI Technological Institute for Superhard and Novel Carbon Materials, Troitsk, Moscow 142190, Russia

<sup>§</sup>Moscow Institute of Physics and Technology, Dolgoprudny 141700, Russia

## Supporting Information

**ABSTRACT:** Results based on *ab initio* density functional calculations indicate that cubic diamond, boron nitride, and many other cubic structures including rocksalt share a general graphitization tendency in ultrathin films terminated by close-packed (111) surfaces. Whereas such compounds often show an energy preference for cubic rather than layered atomic arrangements in the bulk, the surface energy of layered systems is commonly lower than that of their cubic counterparts. We determine the critical slab thickness for a range of systems, below which a spontaneous conversion from a cubic to a layered graphitic structure occurs, driven by surface energy reduction in surface-dominated structures.

**KEYWORDS:** Graphitization, ultrathin films, DFT, *ab initio*, structural phase transition, surface energy



Structural changes at surfaces including atomic relaxation and reconstruction are a manifestation of the driving force to minimize their total free energy.<sup>1,2</sup> Atomic rearrangements are typically moderate at surfaces of semi-infinite systems and in thick slabs so that the energy penalty associated with structural mismatch at the interface between the reconstructed surface and the unreconstructed bulk may be limited. In ultrathin films, surface contribution dominates the total energy, as only a small fraction of atoms experience bulk-like atomic environment. There, a large-scale reconstruction involving not only the topmost layers, but the entire system may yield the most stable structure. Examples of such large-scale atomic rearrangements include the postulated conversion of thin films of layered hexagonal BN to a cubic phase upon fluorination<sup>3</sup> or the conversion of few-layer graphene to diamond upon fluorination or hydrogenation.<sup>4</sup> In general, reduction of the surface energy is driving the reverse process at bare surfaces, leading to graphitization of diamond nanoparticles<sup>5</sup> and nanowires,<sup>6</sup> as well as ultrathin diamond,<sup>7</sup> SiC,<sup>8</sup> and ZnO<sup>9</sup> films. This graphitization scenario, if energetically viable for a large range of compounds, may turn into a valuable bottom-up approach to synthesize hypothetical ultrathin layered structures<sup>10</sup> for nanoelectronics applications in the post-graphene era.

We present results of *ab initio* density functional calculations, which indicate a general graphitization tendency in ultrathin films of cubic compounds. We find that an energy preference for layered honeycomb rather than cubic structures in ultrathin films is rather common, extending from diamond and boron nitride to less obvious cubic structures including silicon carbide, boron phosphide, and rocksalt. Whereas the bulk of such

compounds shows an energy preference for cubic rather than layered atomic arrangements, the surface energy of systems with honeycomb layers is commonly lower than that of their cubic counterparts with close-packed (111) surfaces. Whether the type of crystal bonding is purely covalent, purely ionic, or a combination of the two, the optimum structure of a slab results from an energy competition between the energy preference for a honeycomb structure at the surface and for a cubic atomic arrangement in the bulk. We determine the critical slab thickness for a range of systems, below which a spontaneous conversion from a cubic to a layered graphitic structure occurs, driven by surface energy reduction in surface-dominated structures.

**Results and Discussion.** The inspiration for our study came from structure optimization calculations for ultrathin films with (111) surfaces, constrained to a quasi-2D geometry,<sup>11</sup> which indicated a spontaneous transformation from a cubic to a layered graphitic structure in systems ranging from diamond to rocksalt.<sup>12</sup> The competing cubic and layered graphitic phases for diamond, zincblende, and rocksalt lattices are illustrated in Figure 1. In the following, we investigate the graphitization tendency of ultrathin films of such systems, introduce a simple criterion to judge this tendency, and relate it to the charge redistribution at surfaces.

The tendency of a system to graphitize can be judged by the difference of cohesive energies

**Received:** September 24, 2014

**Revised:** November 10, 2014

**Published:** November 10, 2014

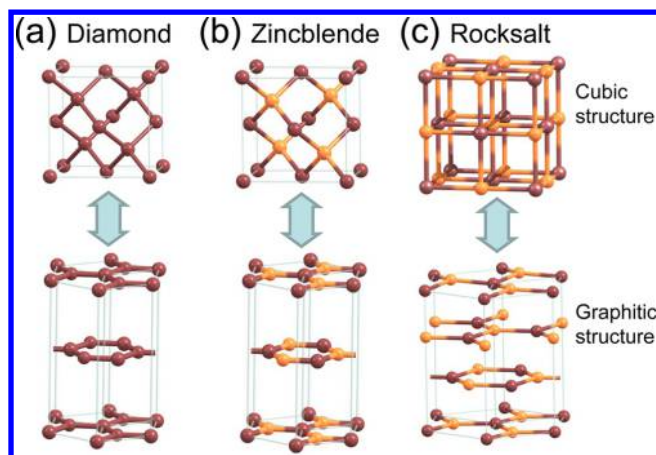


**Figure 1.** Ball-and-stick models of (a) diamond, (b) zincblende, and (c) rocksalt in their native bulk structure (top panels) and their corresponding layered counterparts (bottom panels).

$$\Delta E(\text{bulk}) = E_{\text{cub}}(\text{bulk}) - E_{\text{gra}}(\text{bulk}) \quad (1)$$

in the bulk and

$$\Delta E(N\text{-layer slab}) = E_{\text{cub}}(N\text{-layer slab}) - E_{\text{gra}}(N\text{-layer slab}) \quad (2)$$

in a free-standing  $N$ -layer slab. For the sake of consistency, we subdivide also cubic structures into nominal layers and consider  $N$ -layer slabs with the same number of atoms in the cubic and the graphitic structure. Cohesive energies of bulk and layered structures are taken per unit cell and are listed in Table 1. The

**Table 1.** Calculated Cohesive and Cleavage Energies of Cubic (cub) and Graphitic (gra) Phases of Compounds Presented in Figure 2; All Results Are for the (111) Cleavage Plane;  $N_c$  Is the Critical Number of Layers for Favorable Graphitization According to Figure 2

	$E_{\text{cub}}(\text{bulk})$ (eV/cell)	$E_{\text{gra}}(\text{bulk})$ (eV/cell)	$E_{\text{cub}}(\text{cleave})$ (eV/cell)	$E_{\text{gra}}(\text{cleave})$ (eV/cell)	$N_c$
C	18.18	18.39	3.91	<0.01	$\infty$
BN	17.47	17.57	4.83	0.04	$\infty$
Si	10.84	9.93	2.59	0.89	1
SiC	14.97	14.06	3.31	0.04	3
BP	12.88	12.14	2.66	<0.01	3
NaCl	6.78	6.60	2.34	0.42	11

overbinding of bulk structures, caused by the underbinding of the isolated atoms and common in well-converged DFT calculations, does not affect energy differences. The prevalent energetic preference of the bulk for the cubic rather than a layered graphitic structure can be inferred from data in Table 1 and is indicated by  $\Delta E(\text{bulk}) > 0$ .

As a counterpart to the bulk results, we plot the dependence of the slab cohesive energy difference  $\Delta E(N\text{-layer slab})$  on the number of layers  $N$  in (111) terminated ultrathin films<sup>10</sup> of C, BN, Si, SiC, BP, and NaCl in Figure 2. For  $N \rightarrow \infty$ , these results are consistent with the energetic preference of bulk Si, SiC, BP, and NaCl for the cubic structure, and that of C and BN for the layered graphitic structure. Our most intriguing result is that  $\Delta E$  changes sign in ultrathin films of many of the cubic structures, indicating spontaneous graphitization tendency.

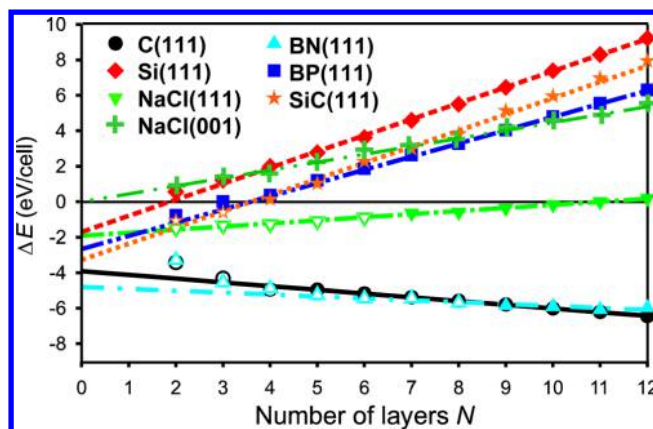


**Figure 2.** Cohesive energy difference  $\Delta E$  of  $N$ -layer slabs with cubic and graphitic structure, with  $\Delta E < 0$  indicating energetic preference for graphitization. Data points are results of DFT calculations. Solid symbols represent structures with locally stable cubic and graphitic phase. Open symbols represent structures with an unstable cubic phase. Lines represent predictions based on eq 5 using quantities listed in Table 1.

The reason for this behavior is the dominant role of the surface energy  $E(\text{surface})$  in the cohesive energy for small values of  $N$ . The behavior of  $\Delta E(N\text{-layer slab})$  in Figure 2 can be explained quantitatively in the following way. For sufficiently thick slabs, the cohesive energy of an  $N$ -layer slab with the cubic structure is given by

$$E_{\text{cub}}(N\text{-layer slab}) = NE_{\text{cub}}(\text{bulk}) - E_{\text{cub}}(\text{cleave}) \quad (3)$$

where  $E_{\text{cub}}(\text{cleave}) = 2E_{\text{cub}}(\text{surface})$  is the cleavage energy of the bulk cubic crystal or twice the surface energy per unit cell. Similarly, the cohesive energy of an  $N$ -layer slab with the layered graphitic structure is given by

$$E_{\text{gra}}(N\text{-layer slab}) = NE_{\text{gra}}(\text{bulk}) - E_{\text{gra}}(\text{cleave}) \quad (4)$$

where  $E_{\text{gra}}(\text{cleave})$  is the cleavage energy corresponding to the interlayer interaction per unit cell of the layered graphitic crystal. Calculated cleavage energies for the systems of interest in cubic as well as layered graphitic structures are listed in Table 1. As expected, the listed cleavage energies are a small fraction of the bulk cohesive energies and in general agreement with published data. They ignore additional energy gain caused by complex surface reconstruction involving large unit cells, which is a small fraction of the surface energy<sup>2</sup> and does not affect our main predictions.

To get a more quantitative description of the graphitization, we may combine eqs 2–4 to

$$\Delta E(N\text{-layer slab}) = N[E_{\text{cub}}(\text{bulk}) - E_{\text{gra}}(\text{bulk})] + [-E_{\text{cub}}(\text{cleave}) + E_{\text{gra}}(\text{cleave})] \quad (5)$$

The linear dependence of  $\Delta E$  on the number of layers, predicted by eq 5, is reproduced amazingly well in Figure 2 down to a few layers. Systems with an energetic preference for the cubic structure in the bulk have a positive slope, and those with a graphitic structure in the bulk have a negative slope. The reason behind the graphitization of most cubic structures in our study is the fact that the cleavage or the surface energy of the graphitic structures is generally lower than that of cubic

structures. This energy difference,  $E_{\text{gra}}(\text{cleave}) - E_{\text{cub}}(\text{cleave})$ , appears as the intercept of the ordinate in Figure 2.

The critical slab thickness for graphitization is determined by the condition  $\Delta E(N_c\text{-layer slab}) = 0$ . In systems with energetic preference for the cubic phase in the bulk, we expect graphitization for  $N < N_c$  layers and may estimate the critical value  $N_c$  using eq 5 from

$$N_c = \frac{E_{\text{cub}}(\text{cleave}) - E_{\text{gra}}(\text{cleave})}{E_{\text{cub}}(\text{bulk}) - E_{\text{gra}}(\text{bulk})} \quad (6)$$

As can be inferred from Figure 2, critical slab thicknesses obtained using the linear extrapolation underlying eq 6 agree generally very well with  $N_c$  values listed in Table 1, which are based on calculated total energy differences in finite slabs, where structural changes at the surface of few-layer systems are considered explicitly. Since only values  $N_c \gtrsim 2$  indicate graphitization, our finding that  $N_c(\text{Si}) = 1$  agrees with the fact that graphitization of free-standing silicon slabs to silicene is unfavorable. We should note that observed silicene layers, which have been stabilized by strong adhesion to a substrate, are not planar, but buckled, indicating their instability and energetic preference for a 3D structure.<sup>13–17</sup> The graphitization condition changes to  $N > N_c$  in systems, where the layered graphitic phase is preferred energetically in the bulk. There, a negative value of  $N_c$  obtained using eq 6 indicates graphitization for all layer thicknesses, equivalent to  $N_c \rightarrow \infty$  in the convention used in Table 1.

We need to reemphasize that our results for the graphitization tendency are given for slabs of the cubic phase terminated by the close-packed (111) surface, which usually has the lowest surface energy. Since the surface energy is typically higher at more open surfaces, corresponding slabs should graphitize at even larger values of  $N_c$ . A notable difference is NaCl, where the surface energy of the (111) surface is higher than that of the more open (001) surface, the typical cleaving plane. Our results in Figure 2 indicate that ultrathin NaCl films with a (001) surface, in contrast to films with a (111) surface, should never graphitize.

Since the graphitization tendency of ultrathin layers depends sensitively on the surface or cleavage energy of bulk structures, we next explore the reasons why the surface energy of graphitic structures is generally lower than that of cubic structures. As we expand later on, the fundamental reason is different in ionic and in covalent solids. In the latter case, formation of a surface by cleaving a bulk structure gives rise to unsaturated bonds and a charge redistribution that is commensurate with the surface energy. To visualize the degree and the spatial extent of the charge redistribution, we considered a region of the bulk structure corresponding to a thick slab, determined the charge density  $\rho(\text{bulk})$  in this region, and set  $\rho = 0$  outside the slab region. Then we truncated the bulk structure to obtain the geometry of an unrelaxed slab and determined the slab charge density  $\rho(\text{slab})$ . Finally, we obtained the charge density difference  $\Delta\rho = \rho(\text{slab}) - \rho(\text{bulk})$  and displayed it in Figure 3.

Inspection of our results in Figure 3 confirms that charge redistribution is confined to the surface region and decays to a vanishing value in the bulk. Comparison between cubic and layered graphitic structures indicates a significantly lower degree of charge redistribution in the latter, reflecting our finding that cleavage and surface energies are lower in layered graphitic than in cubic structures. This is the case not only in covalent systems, but, as seen in Figure 3c, also in ionic systems

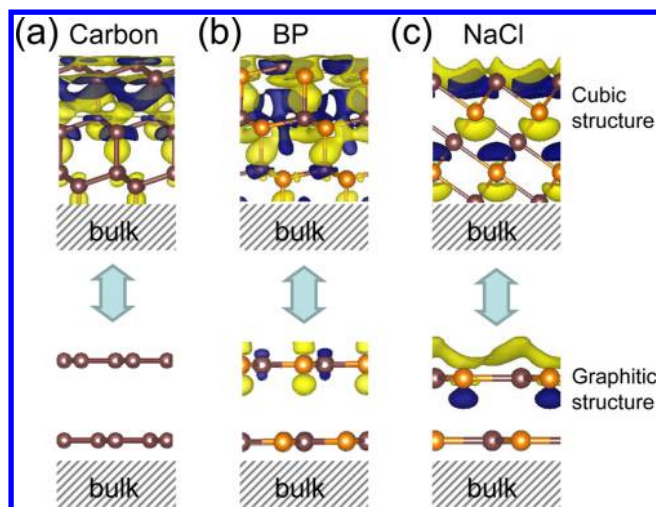


**Figure 3.** Total charge density difference  $\Delta\rho$  between the slab and the bulk structure near the (111) surface of (a) carbon, (b) BP, and (c) NaCl in the bulk cubic (top panels) and the layered graphitic (bottom panels) phase, superposed with the atomic structure. The isosurface values are  $\Delta\rho_{\pm} = \pm 5 \times 10^{-4} \text{ e}/\text{\AA}^3$  to distinguish between regions with electron excess, shown by the dark (blue) isosurfaces, and regions with electron deficit, indicated by the light (yellow) isosurfaces.

like NaCl. We find that the degree of charge redistribution at the surface indeed reflects the relative value of the cleavage energy as listed in Table 1.

Obviously, the physical origin of energetic stabilization and charge redistribution at the surface is different in covalent systems like diamond, in ionic systems such as NaCl, and systems with covalent and ionic bonding contributions such as BP. In covalent systems, as mentioned above, surface energy can be associated with unsaturated dangling bonds. The resulting significant charge redistribution at the surface of diamond is clearly visible in the top panel of Figure 3a. The distribution of  $\Delta\rho$  also indicates that the charge flow in this system is mostly confined to the topmost three layers. In stark contrast to these findings, the charge redistribution caused by cleaving graphite, displayed in the bottom panel of Figure 3a, is significantly smaller. The absence of contours in this figure indicates that the charge density difference between the bulk and the surface lies below  $5 \times 10^{-4} \text{ e}/\text{\AA}^3$ .

The ionic nature of bonding gives rise to a large surface dipole at the (111) surface of the cubic NaCl structure, which is the origin of the large surface energy.<sup>18</sup> As seen in the top panel of Figure 3c, the charge redistribution at the (111) surface of NaCl is significant and, because of the lack of screening, involves more layers than in covalent materials. As an alternative to the bulk cubic structure, we can imagine arranging Na and Cl atoms in charge neutral honeycomb layers that would form a layered structure. As pointed out earlier,<sup>18</sup> the major energetic benefit of the layered graphitic structure of NaCl results from removing the surface dipole component normal to the (111) surface, thus reducing the electrostatic energy penalty. We should note that the same argument applies also to the more stable (001) surface of NaCl with a lower surface dipole moment, which we predict not to graphitize. Our results for  $\Delta\rho$  in the bottom panel of Figure 3c indicate a much smaller degree of charge redistribution in the graphitic layered structure and also a stronger confinement to the narrow surface region, explaining the significant difference

in the cleavage or surface energy between the layered graphitic and the cubic structure, listed in Table 1.

Our results for boron phosphide, shown in Figure 3b, indicate similarities with covalent and ionic systems in Figures 3a,c. For one, cleavage of the cubic phase affects the charge distribution in more surface layers than in purely covalent crystals. We also observe a noticeable charge redistribution upon cleavage of the layered graphitic phase, which is mostly confined to the topmost layer.

We judge the graphitization tendency by total energy differences between cubic and layered systems, as obtained using the PBE total energy functional described in the Methods section. This functional is known to underestimate the van der Waals interactions in layered systems, causing approximately a 1% error in the cohesive energy. Also, spin polarization should provide an extra stabilization by typically a few meV per atom in the surface layer of metallic systems only. Since our numerical results for these energy differences are of the order of several electronvolts per cell according to Figure 2, we ignore these small corrections, as they do not affect the graphitization trend in ultrathin films.

The results presented above have focused on energy differences between two structural phases, but say little about the local stability of these structures or about a way to synthesize them. As mentioned before, the open symbols in the  $\Delta E < 0$  region of Figure 2 indicate instability of the cubic phase and its spontaneous conversion to a layered graphitic phase. For other systems, we find both phases to be locally stable, implying an activation barrier for the conversion. Such energy barriers may be factual or may result from unit cell size and symmetry constraints imposed in our calculations. In an infinite slab with no such constraints, possibly aided by the presence of defects, such activation barriers may be strongly suppressed or even vanish, providing an energetically viable pathway for the structural change. The energetics of the conversion of NaCl from the bulk cubic to the layered graphitic structure is discussed in the Supporting Information.<sup>12</sup>

Since most layered systems are synthesized at nonzero temperatures, the significant quantity to be evaluated and compared is the free energy. Our total energy results for stability differences at  $T = 0$  need to be corrected by also addressing differences in entropy at  $T > 0$ . The formidable task to calculate the entropy including its structural, vibrational, and electronic components as a function of temperature exceeds the scope of this study. Still, by analogy, we may discuss the expected changes in the graphitization trends at nonzero temperatures. The higher flexibility of the less compact layered structures, also evidenced by the emergence of soft flexural modes, causes an additional increase in their structural and vibrational entropy beyond their cubic counterparts. In this case, free energy will favor graphitization also in the interior of the slabs, which is analogous to the well-documented graphitization of cubic diamond at high temperatures. Consequently, we expect the critical slab thickness, below which graphitization occurs, to increase with increasing temperature.

The geometry of samples formed by chemical vapor deposition (CVD) closely resembles the constrained optimized geometry described here. Recent success achieved in CVD synthesis of layered structures including graphene<sup>19</sup> and hexagonal boron nitride<sup>20</sup> indicates that this approach may also be useful to form ultrathin films of other compounds with a layered graphitic structure and that structural selectivity may be

enhanced by a judicious choice of the substrate.<sup>10</sup> An important criterion for the selection of the deposition substrate is the requirement that the substrate–adlayer interface energy should not penalize energetically the formation of a graphitic structure. Free-standing few-layer slabs could then be obtained by mechanical transfer of the deposited structure.

**Conclusions.** In summary, we performed *ab initio* density functional calculations that indicate a general graphitization tendency in ultrathin films of cubic compounds with close-packed (111) surfaces. We found that an energy preference for layered honeycomb rather than cubic structures in ultrathin films is rather common, extending from diamond and boron nitride to less obvious cubic structures including silicon carbide, boron phosphide, and rocksalt. Whereas the bulk of such compounds shows an energy preference for cubic rather than layered atomic arrangements, the surface energy of systems with honeycomb layers is commonly lower than that of their cubic counterparts. Whether the type of crystal bonding is purely covalent, purely ionic, or a combination of the two, the optimum structure of a slab results from an energy competition between the energy preference for a honeycomb structure at the surface and for a cubic atomic arrangement in the bulk. We determined the critical slab thicknesses for a range of systems, below which a spontaneous conversion from a cubic to a layered graphitic structure occurs, driven by surface energy reduction in surface-dominated structures. Finally, we believe that graphitization of ultrathin layers is a rather general phenomenon that is not limited to systems in this study and expect that it will provide a viable route to a bottom-up synthesis of few-layer compounds by CVD.

**Methods.** Our computational approach to learn about the equilibrium structure, stability, and charge distribution in ultrathin films is based on *ab initio* density functional theory (DFT) as implemented in the SIESTA<sup>21</sup> and VASP<sup>22</sup> codes. We used periodic boundary conditions throughout the study, with multilayer structures represented by a periodic array of slabs separated by a 15 Å thick vacuum region. We used the Perdew–Burke–Ernzerhof<sup>23</sup> exchange–correlation functional throughout the study. VASP calculations are based on the projector-augmented wave method, and our SIESTA studies make use of norm-conserving Troullier–Martins pseudopotentials<sup>24</sup> and a double- $\zeta$  basis including polarization orbitals. The plane-wave energy cutoff was set to 180 Ry in SIESTA and 500 eV in VASP. The reciprocal space was sampled by a fine  $k$ -point mesh<sup>25</sup> ranging between  $8 \times 8 \times 3$  and  $6 \times 6 \times 1$   $k$ -points in the Brillouin zone of the primitive unit cell. All geometries have been optimized using the conjugate gradient method,<sup>26</sup> until none of the residual Hellmann–Feynman forces exceeded  $10^{-2}$  eV/Å.

## ■ ASSOCIATED CONTENT

### 📄 Supporting Information

Energetics of the cubic-to-hexagonal transition in NaCl. This material is available free of charge via the Internet at <http://pubs.acs.org>.

## ■ AUTHOR INFORMATION

### Corresponding Author

\*E-mail: [tomanek@pa.msu.edu](mailto:tomanek@pa.msu.edu).

### Notes

The authors declare no competing financial interest.

## ACKNOWLEDGMENTS

This study has been supported by the National Science Foundation Cooperative Agreement #EEC-0832785, titled "NSEC: Center for High-rate Nanomanufacturing". Computational resources have been provided by the Michigan State University High Performance Computing Center and by the Supercomputing Center of the Lomonosov Moscow State University. A.G.K. was supported by a Scholarship from the President of Russia for young scientists and Ph.D. students (competition SP-2013). P.B.S. and A.G.K. acknowledge additional support by the Russian Science Foundation project No. 14-12-01217. P.B.S. acknowledges the hospitality of Michigan State University, where this research was performed.

## REFERENCES

- (1) Somorjai, G. A. *Chemistry in Two Dimensions: Surfaces*; Cornell University Press: Ithaca, NY, 1981.
- (2) Zangwill, A. *Physics at Surfaces*; Cambridge University Press: New York, 1988.
- (3) Zhang, Z.; Zeng, X. C.; Guo, W. *J. Am. Chem. Soc.* **2011**, *133*, 14831–14838.
- (4) Odkhuu, D.; Shin, D.; Ruoff, R. S.; Park, N. *Sci. Rep.* **2013**, *3*, 3276.
- (5) Banhart, F. *Rep. Prog. Phys.* **1999**, *62*, 1181–1221.
- (6) Shang, N.; Papakonstantinou, P.; Wang, P.; Zakharov, A.; Palnitkar, U.; Lin, I.-N.; Chu, M.; Stamboulis, A. *ACS Nano* **2009**, *3*, 1032–1038.
- (7) Kvashnin, A.; Chernozatonskii, L. A.; Yakobson, B. I.; Sorokin, P. B. *Nano Lett.* **2014**, *14*, 676–681.
- (8) Lin, S. S. *J. Phys. Chem. C* **2012**, *116*, 3951–3955.
- (9) Claeysens, F.; Freeman, C. L.; Allan, N. L.; Sun, Y.; Ashfold, M. N. R.; Harding, J. H. *J. Mater. Chem.* **2005**, *15*, 139–148.
- (10) Singh, A. K.; Zhuang, H. L.; Hennig, R. G. *Phys. Rev. B* **2014**, *89*, 245431.
- (11) The growth mechanism of films on selected substrates by chemical vapor deposition (CVD) differs fundamentally from the growth of nanostructures in free space. Whereas aggregation of carbon atoms leads to the formation of fullerenes in free space, layered graphitic structures are formed by CVD on a substrate. Our 2D constrained optimization addresses the latter process.
- (12) See the Supporting Information for the energetics of the cubic-to-hexagonal transition in NaCl.
- (13) Feng, B.; Ding, Z.; Meng, S.; Yao, Y.; He, X.; Cheng, P.; Chen, L.; Wu, K. *Nano Lett.* **2012**, *12*, 3507–3511.
- (14) Vogt, P.; De Padova, P.; Quaresima, C.; Avila, J.; Frantzeskakis, E.; Asensio, M. C.; Resta, A.; Ealet, B.; Le Lay, G. *Phys. Rev. Lett.* **2012**, *108*, 155501.
- (15) Lin, C.-L.; Arafune, R.; Kawahara, K.; Tsukahara, N.; Minamitani, E.; Kim, Y.; Takagi, N.; Kawai, M. *Appl. Phys. Express* **2012**, *5*, 045802.
- (16) Florence, A.; Friedlein, R.; Ozaki, T.; Kawai, H.; Wang, Y.; Yamada-Takamura, Y. *Phys. Rev. Lett.* **2012**, *108*, 245501.
- (17) Meng, L.; Wang, Y.; Zhang, L.; Du, S.; Wu, R.; Li, L.; Zhang, Y.; Li, G.; Zhou, H.; Hofer, W. A.; Gao, H.-J. *Nano Lett.* **2013**, *13*, 685–690.
- (18) Freeman, C. L.; Claeysens, F.; Allan, N. L.; Harding, J. H. *Phys. Rev. Lett.* **2006**, *96*, 066102.
- (19) Reina, A.; Jia, X.; Ho, J.; Nezich, D.; Son, H.; Bulovic, V.; Dresselhaus, M. S.; Kong, J. *Nano Lett.* **2009**, *9*, 30–35.
- (20) Song, L.; Ci, L.; Lu, H.; Sorokin, P. B.; Jin, C.; Ni, J.; Kvashnin, A. G.; Kvashnin, D. G.; Lou, J.; Yakobson, B. I.; Ajayan, P. M. *Nano Lett.* **2010**, *10*, 3209–3215.
- (21) Artacho, E.; Anglada, E.; Dieguez, O.; Gale, J. D.; Garcia, A.; Junquera, J.; Martin, R. M.; Ordejon, P.; Pruneda, J. M.; Sanchez-Portal, D.; Soler, J. M. *J. Phys.: Condens. Matter* **2008**, *20*, 064208.
- (22) Kresse, G.; Furthmüller, J. *Phys. Rev. B* **1996**, *54*, 11169–11186.
- (23) Perdew, J. P.; Burke, K.; Ernzerhof, M. *Phys. Rev. Lett.* **1996**, *77*, 3865–3868.
- (24) Troullier, N.; Martins, J. L. *Phys. Rev. B* **1991**, *43*, 1993.
- (25) Monkhorst, H. J.; Pack, J. D. *Phys. Rev. B* **1976**, *13*, 5188–5192.
- (26) Hestenes, M. R.; Stiefel, E. J. *Res. Natl. Bur. Stand.* **1952**, *49*, 409–436.